Optimal Operational Planning of Distribution Systems: A Neighborhood Search-based Matheuristic Approach

Jairo Yumbla[a], Juan M. Home-Ortiz[bc], Tiago Pinto[d], João P. S. Catalão[e], José R. S. Mantovani[a]

[a]*Department of Electrical Engineering, São Paulo State University, Avenida Brasil 56, Centro, 15385-000, Ilha Solteira, SP, Brazil.*

[b]*Polytechnic School of the University of São Paulo, 05508-010 São Paulo, SP.*

[c]*University of Campinas, Department of Systems and Energy, Campinas, São Paulo, CEP13083-852, Brazil.*

[d]*University of Trás-os-Montes and Alto Douro*, and, INESC-TEC, Quinta de Prados, 5000-801, Vila Real, Portugal

[e]*Faculty of Engineering of the University of Porto and the Research Center for Systems and Technologies (SYSTEC), 4200-465 Porto, Portugal*

E-mail addresses: jairo.yumbla@unesp.br (Jairo Yumbla), juan.home@unesp.br (Juan M. Home-Ortiz) , tiagopinto@utad.pt (Tiago Pinto), catalao@fe.up.pt (João P. S. Catalão), mant@dee.feis.unesp.br (José R. S. Mantovani).

1. ABSTRACT

This study proposes a strategy for short-term operational planning of active distribution systems to minimize operating costs and greenhouse gas (GHG) emissions. The strategy incorporates network reconfiguration, switchable capacitor bank operation, dispatch of fossil fuel-based and renewable distributed energy resources, energy storage devices, and a demand response program. Uncertain operational conditions, such as energy costs, power demand, and solar irradiation, are addressed using stochastic scenarios derived from historical data through a k-means technique. The mathematical formulation adopts a stochastic scenario-based mixed-integer second-order conic programming (MISOCP) model. To handle the computational complexity of the model, a neighborhood-based matheuristic approach (NMA) is introduced, employing reduced MISOCP models and a memory strategy to guide the optimization process. Results from 69 and 118-node distribution systems demonstrate reduced operational costs and GHG emissions. Moreover, the proposed NMA outperforms two commercial solvers. This work provides insights into optimizing the operation of distribution systems, yielding economic and environmental benefits.

Keywords:
Demand response, energy storage devices, greenhouse gas emissions mitigation, matheuristic, mixed-integer second-order conic programming, network reconfiguration.

2. NOMENCLATURE

Sets and indices

$i, j/ki, ij$	Indices for nodes/branches;
Ω_b	Set of branches;
Ω_{dg}	Set of nodes with dispatchable generators installed;
Ω_{esd}	Set of nodes with energy storage devices installed;
Ω_n	Set of nodes;
Ω_{pv}	Set of nodes with photovoltaic panels installed;

Ω_s	Scenarios I and II such that: $s \in \{1, 2\}$;
Ω_{scb}	Set of nodes with switchable capacitors bank installed;
Ω_{ss}	Set of substation nodes;
Ω_t	Set of periods of the day such that: $t \in \{0, \dots, 11\}$;

Parameters

c_h^{energy}	Historical hourly measurements of the cost of energy
$C_{t,s}^{energy}$	Price per unit of energy in scenario c;
C^{tax}	Penalty per ton of CO_2 emitted;
e^{ss}, e^{dg}	CO_2 emission factor from the substation and dispatchable generators, respectively;
g_h	Historical hourly measurements of solar irradiation;
$G_{t,s}$	Solar irradiation in scenario c;
$\overline{I_{ij}}$	Maximum thermal capacity of the line ij;
$\overline{n_i}^{scb}$	Number of installed capacitor banks at node i;
$NOCT_i$	Nominal operating cell temperature of PV at node i;
$P_{i,t,s}^d, Q_{i,t,s}^d$	Active/reactive power demand at load node i;
$\underline{P_{i,t,s}^{esd^{ch}}}, \overline{P_{i,t,s}^{esd^{ch}}}$	Lower/Upper limits of charge of ESD connected at node i;
$\underline{P_{i,t,s}^{esd^{dch}}}, \overline{P_{i,t,s}^{esd^{dch}}}$	Lower/Upper limits of discharge of ESD connected at node i;
P_i^{std}	Power under standard conditions of PV at node i;
Q_i^{fcb}	Reactive power injected by the fixed capacitor at node i;
q_i^{scb}	Reactive power capacity of each unit of an SCB;
R_{ij}, X_{ij}	Resistance and reactance of branch ij;
$\overline{S_i^{ss}}, \overline{S_i^{dg}}$	Maximum capacity of SS/DG at node i;
$T_{t,s}$	Duration of each analysis period;
$T_{amb}, T_{i,t,s}^{cell}$	Ambient temperature; and temperature of PV at node i;
$\underline{V}, \overline{V}$	Min./max. limits of voltage's magnitude in nodes;
Z_{ij}^{sqr}	Squared impedance of branch ij;
$\mathfrak{Z}^{dr}$	Percentage of the maximum decreases allowed in loads to apply the DRP;
δ_i	Power/temperature coefficient of PV at node i;
$\xi_i^{esd^{ch}}, \xi_i^{esd^{dch}}$	Charge/discharge efficiency of ESDs;
ζ_i^{esd}	Self-discharge rate of ESDs;
$\mathfrak{f}_{t,s}$	Demand factor, scenario t,s;
θ_i^{pf}	Power factor of load connected at node i;
$\varphi_i^{c/dg}, \varphi_i^{i/dg}$	Capacitive/inductive power factors of DG unit at node i;
$\varphi_i^{c/pv}, \varphi_i^{i/pv}$	Capacitive/inductive power factors of PV unit at node i;
$\eta, \overline{\eta}^{scb}, \overline{\eta}^{esd}$	Maximum changes on SCBs/ESDs while neighborhood search;
$\pi_{t,s}^{energy}, \pi^{emis}, \pi^{ens}$	Cost parameters of energy, CO_2 emissions and energy not supplied, respectively;

π^{dr}	Discount rate of energy cost when DRP is applied;
$\rho_{t,s}$	Probability of occurrence of scenario c;
$\Delta_i^{scb}, \Delta_i^{esd}$	Maximum allowed maneuvers on SCBs/ESDs;

Continuous variables

$C_{t,s}^{dr}, C_{t,s}^{emis}, C_{t,s}^{ens}, C_{t,s}^{loss}$	Cost of demand response, CO_2 emissions, energy not supplied, and energy losses in scenario t,s, respectively;
$E_{i,t,s}^{esd}$	Stored energy in ESD;
$e_{i,t,s}^{esd^{dch}}, e_{i,t,s}^{esd^{ch}}$	Auxiliary variables to account for maneuvers on ESDs;
$I_{ij,t,s}^{sqr}$	Square of current flow in branch ij;
$P_{ij,t,s}, Q_{ij,t,s}$	Active and reactive power flow in branch ij, scenario t,s;
P_i^d, Q_i^d	Active and reactive maximum load connected at node i;
$P_{i,t,s}^{dg}, Q_{i,t,s}^{dg}$	Active and reactive power injection by DG units;
$P_{i,t,s}^{d/dr}, Q_{i,t,s}^{d/dr}$	Active and reactive demand after DRP application;
$P_{i,t,s}^{esd^{ch}}, P_{i,t,s}^{esd^{dch}}$	Charge/discharge power of ESD connected at node i;
$P_{i,t,s}^{ens}$	Not supplied power at node i;
$P_{i,t,s}^{pv}, Q_{i,t,s}^{pv}$	Active and reactive power injection by PV units;
$P_{i,t,s}^{ss}, Q_{i,t,s}^{ss}$	Active and reactive power injection by substations;
$P_{i,t,s}^{tou^+}, P_{i,t,s}^{tou^-}$	Increase/decrease of active load when TOU-DRP is applied at node i;
$Q_{i,t,s}^{scb}$	Reactive power injected by an SCB at node i;
$n_{i,t,s}^{+}, n_{i,t,s}^{-}$	Auxiliary variables to account for increase/decrease maneuvers on SCB installed at node i;
$V_{i,t,s}^{sqr}$	Square of voltage at node i;
$\mu_{ij,t,s}$	Slack variable for voltage calculation;
Ψ	Operational cost, Objective function;

Integer variables

$e_{i,t,s}^{esd}$	Binary variable to state the charge or discharge of the ESD connected at node i;
k_{ij}	Binary variable to indicate the status of branch ij ;
$n_{i,t,s}^{scb}$	Number of connected capacitors in an SCB during scenario t,s;
β_{ij}	Binary variable to indicate j is the parent node of i;
$\varsigma_{i,t,s}^{tou}$	Binary variable to indicate the application or not of DRP at node i;

3. INTRODUCTION

In response to the growing climate crisis, nations globally are actively incorporating distributed energy resources (DERs) to diminish the reliance on fossil fuels [1], [2]. The increasing relevance of low-carbon policies further complicates the operational planning of distribution systems (DSs), posing challenges in maintaining balance due to demand variability and uncertainties from renewable energy resources (RESs) [3], [4]. Simultaneously, carbon emission trading policies, leveraging financial incentives, emerge as highly effective in mitigating emissions [5]. Achieving low-carbon operational planning for DSs in this

context requires effective solutions to manage uncertainties, a critical aspect in meeting carbon neutrality targets [6].

The optimal operation of DSs (OODS) is a well-known problem that aims to optimize the scheduling and operational state of DERs and other network resources over a planning horizon [7], [8]. In this regard, it is crucial to consider various available technologies in optimizing the DSs operation such as dispatchable generators (DGs), photovoltaic generators (PVs), capacitor banks (CBs), switched capacitor banks (SCBs), and energy storage devices (ESDs). Furthermore, a short-term topology reconfiguration planning (i.e. a seasonal topology plan), based on renewable source patterns from historical data, can enhance DSs operation. Similarly, demand response programs (DRPs) appear to support the DSs performance by allowing consumers to actively participate in deregulated electricity markets. DRPs involve modifying load consumption patterns to reduce peak demand periods, incentivizing user participation through rewards [9]. On the other hand, objective functions in OODS problem typically involve minimizing energy purchased cost, power losses, voltage deviation, DGs, and ESDs operation costs. Given the significance of DERs in the low-carbon transition [6], emerging considerations include minimizing greenhouse gas (GHG) emissions, DRPs incentives, load shedding, and maximizing social welfare [5], [6], [10], [11], [12]. Finally, it is important to mention that combining the above elements in a mathematical model, results in a big and heavy problem from a computational point of view. Consequently, this work explores a matheuristic approach, which combines mathematical programming and heuristic techniques to handle complex optimization problems and has been applied in several areas including power systems optimization [13], [14], [15].

The specialized literature encompasses various studies on optimal distribution system operation, for example, Reference [1] introduces a collaborative framework for multi-stakeholder DERs, utilizing a cascading algorithm to achieve a win-win situation. Moreover, carbon tax and demand response to electric and heat loads are applied in the framework, and the problem is solved through an analytical target cascading algorithm. The authors in [4] focus on DERs optimization for energy independence in the Canarian Islands, employing a transient system simulation tool for simulation. The work concludes by encouraging the participation of stakeholders to achieve net/nearly zero energy goals for island communities. In [5], a two-stage low-carbon scheme of energy dispatch based on active demand side management (DSM) is proposed considering different types of generation (coal, gas-fired, hydro, wind, and PV), ESDs. The paper concludes with a clear carbon emission reduction by the application of DSM. A similar work is proposed in [6] where the dual consensus alternating direction multiplier algorithm is proposed to solve the problem. Results show a reduction of carbon emissions by 14%. Reference [8] addresses the optimal operation of DSs considering volt/var control, using an evolutionary algorithm to minimize operational costs. Tap change costs are found to be crucial for conservation voltage reduction goals. In [10], a mixed-integer second-order cone programming model is presented to determine the optimal operation of DSs considering the influence of energy storage devices and other DERs, such as DGs, CB, SCB on-load tap-changers. The authors in [11] propose a mixed-integer linear programming model for the optimal operation of DGs, ESDs, and wind turbines. The problem is treated by the CPLEX solver, and uncertainty considerations provide better solutions than a deterministic treatment. Reference [12] introduces a two-stage stochastic model for an energy hub with the presence of ESDs. Furthermore, demand response is applied, and the problem is treated by both real and binary-coded genetic algorithms, offering a comprehensive overview of studies applying various strategies for optimal distribution system operation.

Distribution network reconfiguration (DNR) stands as a robust strategy to enhance the operation of dynamic and active DSs [16]. In the specialized literature, numerous studies have explored this topic using mathematical programming and metaheuristic algorithms [17], [18]. For instance, a convex-based DNR model employing mixed-integer second-order conic programming (MISOCP) was introduced in [19], offering accurate power loss calculations. Subsequent research has further developed conic models to address the DNR problem. Some examples include the big-M method for power loss minimization [20], a joint formulation of DNR and capacitor bank (CB) placement [21], and a mixed-integer linear programming (MILP) model that separates variables into real and imaginary parts [22]. While mathematical programming approaches face computational limitations with increasing problem complexity, metaheuristics, such as tabu search (TS), simulated annealing, evolutionary algorithms, genetic algorithms, and differential evolution, have gained traction for solving the DNR problem [23]. However, these approaches do not guarantee optimal global solutions and rely on the developer's expertise.

As an additional strategy, DRPs allow consumers to actively participate in deregulated electricity markets. They involve modifying load consumption patterns to reduce peak demand periods, and incentivizing user participation through rewards [9]. These programs offer flexibility and positively impact technical and economic aspects [24]. In the literature, various multi-objective reconfiguration models incorporating time-of-use DRPs (TOU-DRP) have been proposed [9], [25]. Additionally, stochastic multi-objective approaches considering dispatchable, wind, and solar generation, along with DRPs and ESDs, have been explored in [26], where Monte Carlo simulations are used to account for parameter uncertainties.

Parameter uncertainties are a crucial consideration in addressing challenges related to the optimal operation of DSs. Various strategies have been proposed in the literature, where one of the most applied methods are the scenario-based ones whose are obtained from historical data [26]. In the context of DNR, it becomes essential to incorporate the influence of stochastic parameters and the impact of installed DERs along the feeders. For example, a day-ahead reconfiguration with a generation scheduling model that incorporates biomass, fuel cells, small hydro, geothermal, solar, wind, and electric vehicles as special loads was presented in [27]. The study in [9] quantifies a significant reduction in carbon emissions after network reconfiguration, highlighting the proportional relationship between emissions and losses. Another study proposed a multi-objective optimization model considering DERs and electric vehicles, solved using the beetle swarm algorithm and scenario reduction with the k-means method [28].

Addressing the OODSs problem, considering all the summarized strategies, results in high complexity that is challenging for mathematical programming and metaheuristic approaches. Recognizing these limitations, the matheuristic concept emerges as a promising solution. Matheuristic algorithms uniquely blend mathematical programming and heuristic techniques to effectively tackle intricate optimization problems. In power systems, variable neighborhood search-based matheuristic algorithms have been employed for DS expansion planning [29] and optimal power flow in transmission systems [30]. A neighborhood structure-based matheuristic approach was used in [31] to solve the DNR problem, but it did not consider energy storage devices or a demand response program. Notably, the methods proposed in [29], [30], [31] outperformed commercial solvers.

Building upon the aforementioned background of topics and strategies, this study aims to ascertain the optimal operational planning of modern dynamic and active DSs. The focus includes network reconfiguration, optimal scheduling of active devices like dispatchable DGs and energy storage, along with the integration of a demand response program. Uncertainties in DS operational planning are

considered by representing a typical day of a specific season through a set of stochastic scenarios that capture uncertain behavior of energy cost, power demand, and solar irradiation. The mathematical formulation of the problem is presented as a stochastic MISOCP model and an efficient matheuristic approach is introduced to address this complex problem. TABLE 1 summarizes the differences between this paper and the state of the art of the problem of optimal operation planning of active distribution systems. The main contributions of this work are explained as follows:

- **Novel Matheuristic Algorithm:** Introducing a pioneering matheuristic algorithm that seamlessly integrates mathematical programming and heuristic techniques. This combination enables the effective operational optimization of complex DS, considering diverse operational aspects.
- **Focus on Modern DS Challenges:** Emphasizing specific attention to challenges inherent in modern DSs, such as network reconfiguration, dispatch of Distributed Energy Resources, Demand Response Programs, and Energy Storage Devices. These aspects might not have been comprehensively explored in existing literature.
- **Extensible Neighborhood Structures:** Developing a set of extensible neighborhood structures based on MISOCP models. These structures enhance the flexibility of the approach, making it applicable to various DS optimization problems.
- **Case Studies and Performance Evaluations:** Conduct targeted case studies and rigorous over commercial solvers. This practical demonstration underscores the effectiveness of the contributions.

In summary, this work advances the field of DS operational planning by integrating matheuristics, addressing the distinctive challenges of modern DSs, accommodating uncertainties, and providing performance evaluations. These contributions, coupled with the unique features of the proposed approach,

TABLE 1. Taxonomy Table of Optimal Operational Planning Strategy for Distribution Systems.

	Uncertainties	Renewable generation	Operational cost minimization	GHG minimization	DGs schedule	SCBs schedule	ESDs schedule	Demand response program	Reconfig.	Mathematical model
[1]	--	✓	✓	--	✓	--	✓	✓	--	MINLP
[5]	--	✓	✓	✓	✓	--	✓	✓	--	MINLP
[6]	--	✓	✓	✓	✓	--	✓	✓	--	MINLP
[7]	--	--	--	--	✓	--	--	--	✓	MISOCP
[8]	--	--	✓	--	--	✓	--	--	✓	MISOCP
[9]	✓	--	--	--	--	--	--	✓	✓	MINLP
[11]	✓	✓	✓	--	✓	--	✓	--	--	MINLP
[12]	✓	✓	✓	✓	--	--	✓	✓	--	NLP
[13]	✓	✓	✓	--	✓	--	✓	✓	✓	MINLP
[14]	--	✓	✓	--	✓	--	--	✓	✓	MISOCP
[15]	✓	✓	--	--	--	--	--	--	✓	MINLP
[16]	--	--	--	--	--	--	--	✓	✓	MINLP
[17]	✓	✓	✓	--	--	--	✓	✓	✓	MIQCP
[18]	--	✓	✓	✓	--	--	✓	✓	✓	MILP
[24]	✓	✓	✓	✓	✓	✓	--	--	✓	MISOCP
This work	✓	✓	✓	✓	✓	✓	✓	✓	✓	MISOCP

set it apart from existing literature, offering insights for the management and optimization of distribution systems. The subsequent sections of the paper delve into the details of the proposed MISOCP model, the matheuristic algorithm, and present results obtained for the 69-bus and 118-bus distribution systems. Finally, the study concludes by summarizing key findings.

4. PROBLEM FORMULATION

4.1. Uncertainty

The incorporation of distributed energy resources (DERs) in modern power grids necessitates modeling non-deterministic parameters such as energy cost, load demand, and RESs [32]. Among various techniques, clustering methods are suitable and easy-to-implement alternatives [2], [33], [34], [35]. These methods group a set of observations into clusters, extracting the most representative information from extensive data sets [36]. This work chose the k-means method due to its suitability and proven performance in modeling uncertainty parameters in power systems [37].

As depicted in Fig. 1, the measurements represent the hourly values of the parameters during the autumn of 2014 (93 days), in the São Paulo region of Brazil. These parameters are the normalized values (p.u.) for energy cost, demand, and solar irradiation. The k-means algorithm is applied to reduce the set of observations at each day's period into clusters using the following steps:

Step 1- Daily curves: The entire dataset is divided into blocks of 24 hours, representing 93 daily profiles.

Step 2- Period Definition: Each block is further divided into twenty-four equal periods.

Step 3- The k-means process is applied to each of the twenty-four periods, dividing the 93 samples into two clusters. The centroids of these clusters represent the parameter values for scenarios I and II. As these are stochastic scenarios, their probability of occurrence depends on the number of samples forming the cluster. Consequently, a vector is generated for each scenario $s \in \{1,2\}$ of period $t \in \{0, 1, 2, \dots 23\}$, containing the energy cost, demand, solar irradiation, and probability. Thus, the final structure of the scenario vector is $\left[C_{t,s}^{energy} \quad \mathfrak{f}_{t,s} \quad G_{t,s} \quad \rho_{t,s}\right]$.

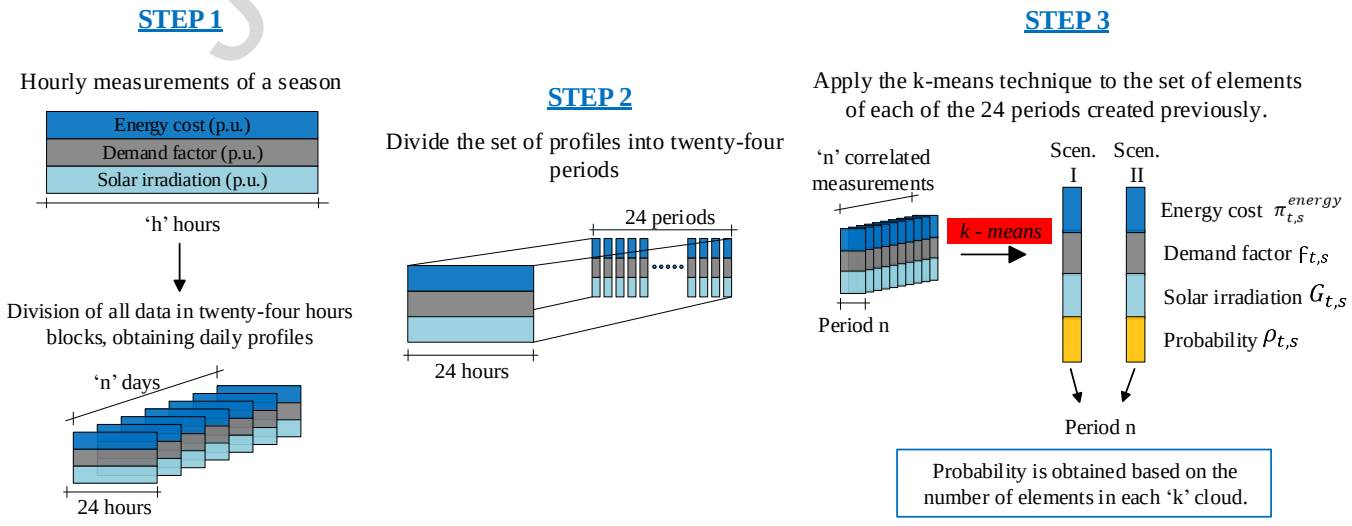

Fig. 1 Stochastic scenario generation approach.

4.2. Objective Function

The proposed model aims to determine an operating state that reduces the operational cost of the system over a planning horizon. Thus, the objective function Ψ, presented in (1), minimizes the active power losses, CO2 emissions, rewards for the demand response program, and energy not supplied to loads.

$$Min\ \Psi = \sum_{t\in\Omega_t}\sum_{s\in\Omega_s} \rho_{t,s}\, T_{t,s}\left(C_{t,s}^{loss} + C_{t,s}^{emis} + C_{t,s}^{dr} + C_{t,s}^{ens}\right) \tag{1}$$

Where:

$$C_{t,s}^{Loss} = \pi_{t,s}^{energy} \sum_{ij\in\Omega_b} R_{ij} I_{ij,t,s}^{sqr} \tag{2}$$

$$C_{t,s}^{emis} = \pi^{emis}\left(\sum_{i\in\Omega_{ss}} e^{ss} P_{i,t,s}^{ss} + \sum_{i\in\Omega_{dg}} e^{dg} P_{i,t,s}^{dg}\right) \tag{3}$$

$$C_{t,s}^{dr} = \pi^{dr}\cdot\pi_{t,s}^{energy} \sum_{i\in\Omega_b} P_{i,t,s}^{tou^+} \tag{4}$$

$$C_{t,s}^{ens} = \pi^{ens} \sum_{i\in\Omega_b} P_{i,t,s}^{ens} \tag{5}$$

The power loss cost of the system is determined in (2). The cost of gas emissions from the sub-transmission system and dispatchable fossil fuel-based DG units of the system is estimated in (3). The cost for demand response application is a total discount in tariff due to changes in the schedule of energy supply. The system operator can supply energy to some type of load at any convenient period, meeting the daily energetic requirements of the customer. Additionally, the customer would receive a percentage discount on energy prices (π^{dr}), at the period defined by the system operator. This can be an advantage at periods of peak load to reduce an allowed percentage of demand. This concept is addressed in (4) where $P_{i,t,s}^{tou^+}$ is the power that is being delivered to customer. Finally, equation (5) corresponds to a possible share of energy not supplied at any load bus to avoid constraint violation.

4.3. Operational State of the System

The DS's steady state is assessed through the following second-order conic programming model, (6)–(10).

$$\sum_{ki\,\epsilon\,\Omega_b} P_{ki,t,s} - \sum_{ij\,\in\,\Omega_b}\left(P_{ij,t,s} + R_{ij} I_{ij,t,s}^{sqr}\right) + P_{i,t,s}^{ss} + P_{i,t,s}^{dg} + P_{i,t,s}^{pv} + P_{i,t,s}^{esd^{dch}} - P_{i,t,s}^{esd^{ch}} = P_{i,t,s}^{d/dr} \tag{6}$$

$$\sum_{ki\,\epsilon\,\Omega_b} Q_{ki,t,s} - \sum_{ij\,\in\,\Omega_b}\left(Q_{ij,t,s} + X_{ij} I_{ij,t,s}^{sqr}\right) + Q_{i,t,s}^{ss} + Q_{i,t,s}^{dg} + Q_i^{fcb} + Q_{i,t,s}^{scb} + Q_{i,t,s}^{pv} = Q_{i,t,s}^{d/dr} \tag{7}$$

$$\forall\, i \in \Omega_n, \forall\, t \in \Omega_t, \forall\, s \in \Omega_s$$

$$V_{i,t,s}^{sqr} - V_{j,t,s}^{sqr} + \mu_{ij,t,s} = 2\left(R_{ij} P_{ij,t,s} + X_{ij} Q_{ij,t,s}\right) + Z_{ij}^{sqr} I_{ij,t,s}^{sqr} \tag{8}$$

$$\left|\mu_{ij,t,s}\right| \le (\overline{V}^2 - \underline{V}^2)(1 - k_{ij}) \tag{9}$$

$$I_{ij,t,s}^{sqr} V_{j,t,s}^{sqr} \geq P_{ij,t,s}^{2} + Q_{ij,t,s}^{2} \tag{10}$$

$$\forall\, ij \in \Omega_b\ ,\forall\, t \in \Omega_t,\forall\, s \in \Omega_s$$

$$0 \leq I_{ij,t,s}^{sqr} \leq \overline{I_{ij}}^{2} \cdot k_{ij} \tag{11}$$

$$\underline{V}^{2} \leq V_{i,t,s}^{sqr} \leq \overline{V}^{2} \tag{12}$$

$$P_{i,t,s}^{ss\ 2} + Q_{i,t,s}^{ss\ 2} \leq \overline{S_i^{ss}}^{2} \mid i \in \Omega_{ss} \tag{13}$$

$$\forall\, i \in \Omega_n,\forall\, ij \in \Omega_b,\forall\, t \in \Omega_t,\forall\, s \in \Omega_s$$

Constraints (6) and (7) represent the active and reactive power balances. Net power injected at i must satisfy the demand level in each scenario. The load at node i ($P_i^{d/dr}$ and $Q_i^{d/dr}$) are the values obtained after DRP has been applied. Constraint (8) calculates the voltage drop along a branch. As presented in (9), variable $\mu_{ij,t,s}$ provides a degree of freedom between ($\overline{V}^2 - \underline{V}^2$) in the voltage calculation when the branch ij is open ($k_{ij} = 0$). The second-order conic constraint (10) states the square current flow magnitude. At the steady state point, this constraint it is equivalent to equality, as explained in [38].

Constraints related to the operational limits of the system are presented in (11)-(13). Constraint (11) represents the current limit through a branch. Constraint (12) holds the voltage regulation limits of the system, and finally, constraint (13) determines that supplied complex power by the substation must be within its maximum capacity.

4.4. Radiality Constraints

The radiality of DSs can be modeled as a spanning tree of a graph with a substation as the root, load nodes are vertices, and branches are edges [19]. The mathematical model uses the binary variables β_{ij} and β_{ji} to indicate if node j is the parent of node i, or vice versa, and the binary variable k_{ij} that indicates the operating state (open/closed) of the branch ij. Based on constraints (14)-(17), if the branch ij is part of a spanning tree, it implies that $k_{ij} = 1$. When the above occurs, either β_{ij} or β_{ji} must be 1 where $\beta_{ij} = 1$, defines that j is the parent node of i, otherwise $\beta_{ji} = 1$, which defines that i is the parent node of j.

$$\beta_{ij} + \beta_{ji} = k_{ij} \tag{14}$$

$$\sum_{j \in \Omega_n \mid ij \in \Omega_b \text{ or } ji \in \Omega_b} \beta_{ij} = 1 \tag{15}$$

$$\beta_{ij} = 0 \quad \mid j \in \Omega_{ss} \tag{16}$$

$$\beta_{ji} = 0 \quad \mid i \in \Omega_{ss} \tag{17}$$

$$\beta_{ij}, \beta_{ji}, k_{ij} \in \{0,1\}$$

$$\forall\, ij \in \Omega_b$$

If a branch connecting nodes i and j is closed, i.e., $k_{ij} = 1$, constraint (14) sets one of these nodes as the parent. Constraint (15) forces load nodes to have only one parent node. Constraints (16) and (17) prevent substation nodes from having a parent node.

4.5. Distributed Generation

The proposed model considers the presence of fossil fuel-based DGs and photovoltaic generation (PVs). The behavior of fossil fuel-based DGs is presented in (18)–(20).

$$\left(P_{i,t,s}^{dg}\right)^2 + \left(Q_{i,t,s}^{dg}\right)^2 \leq \left(\overline{S_i^{dg}}\right)^2 \tag{18}$$

$$P_{i,t,s}^{dg} \geq 0 \tag{19}$$

$$-P_{i,t,s}^{dg} \cdot tan\left(cos^{-1}\varphi_i^{c/dg}\right) \leq Q_{i,t,s}^{dg} \leq P_{i,t,s}^{dg} \cdot tan(cos^{-1}\varphi_i^{i/dg}) \tag{20}$$

$$\forall\, i \in \Omega_{dg}, \forall\, t \in \Omega_t, \forall\, s \in \Omega_s$$

The active and reactive power injected by DGs is limited by power capacity $\overline{S_i^{dg}}$ (18). The machine can inject active power (19) and either inject or absorb reactive power (20). This injection or absorption is limited by the capacitive $\varphi_i^{c/dg}$ and inductive $\varphi_i^{i/dg}$ machine's power factors.

$$P_{i,t,s}^{pv} = P_i^{std}\left\{\frac{G_{t,s}}{1000}\left[1 + \delta_i\left(T_{i,t,s}^{cell} - 25\right)\right]\right\} \tag{21}$$

$$-P_{i,t,s}^{pv} \cdot \tan\left(cos^{-1}\varphi_i^{c/pv}\right) \leq Q_{i,t,s}^{pv} \leq P_{i,t,s}^{pv} \cdot \tan(cos^{-1}\varphi_i^{i/pv}) \tag{22}$$

$$T_{i,t,s}^{cell} = T_{amb} + \left(\frac{NOCT_i - 20}{800}\right) G_{t,s} \tag{23}$$

$$\forall\, i \in \Omega_{pv}, \forall\, t \in \Omega_t, \forall\, s \in \Omega_s$$

For PV units, the power injection depends on the solar irradiation available in each scenario [39]. Therefore, active and reactive power injected by PV units are determined in (21) and (23), respectively.

4.6. Capacitor banks constraints

Constraints (21)–(27) present the mathematical model for the operation of SCBs.

$$Q_{i,t,s}^{scb} = n_{i,t,s}^{scb} \cdot q_i^{scb} \tag{24}$$

$$0 \leq n_{i,t,s}^{scb} \leq \overline{n}_i^{scb} \tag{25}$$

$$n_{i,t_{ini},s}^{scb} = n_{i,t_{end},s}^{scb} \quad | \quad t_{ini} = 0 \;\&\; t_{end} = 23 \tag{26}$$

$$\sum_{t\in\Omega_t}\sum_{s\in\Omega_d} n_{i,t,s}^{+} + n_{i,t,s}^{-} \leq \Delta_i^{scb} \tag{27}$$

$$n_{i,t,s}^{scb} - n_{i,t-1,s}^{scb} = n_{i,t,s}^{+} - n_{i,t,s}^{-} \tag{28}$$

$$n_{i,t,s}^{+} \geq 0 \tag{29}$$

$$n_{i,t,s}^{-} \geq 0 \tag{30}$$

$$\forall\, i \in \Omega_{scb}, \forall\, t \in \Omega_t, \forall\, s \in \Omega_S$$

The total power injection of the SCB at node i, is calculated by (24) and depends on the number of active CB modules. The number of active CB modules in a period is limited by constraint (25). Equation (26) maintains the equality between the number of connected units for the first and last periods of the day. Constraints (27)-(30) limit the daily switching operations for the SCB at node i. At each node with a SCB $n_{i,t,s}^{+}$, and $n_{i,t,s}^{-}$ are positive variables that count the variation in the number of connected units between

two consecutive periods, as stated in constraint (28). Finally, (29) and (30) allow the variables $n^{+}_{i,t,s}$ and $n^{-}_{i,t,s}$ to take positive values only.

4.7. Energy Storage Devices

The ESDs' operation is modeled in (31)-(37), as presented in [10].

$$e^{esd}_{i,t,s}\underline{P^{esd^{dch}}_{i,t,s}} \leq P^{esd^{dch}}_{i,t,s} \leq e^{esd}_{i,t,s}\overline{P^{esd^{dch}}_{i,t,s}} \tag{31}$$

$$(1-e^{esd}_{i,t,s})\underline{P^{esd^{ch}}_{i,t,s}} \leq P^{esd^{ch}}_{i,t,s} \leq (1-e^{esd}_{i,t,s})\overline{P^{esd^{ch}}_{i,t,s}} \tag{32}$$

$$E^{esd}_{i,t,s} = E^{esd}_{i,t-1,s} + T_{t,s}\xi^{esd^{ch}}_{i}P^{esd^{ch}}_{i,t,s} - \frac{T_{t,s}}{\xi^{esd^{dch}}_{i}}P^{esd^{dch}}_{i,t,s} - \zeta^{esd}_{i}E^{esd}_{i,t,s} \tag{33}$$

$$\underline{E^{esd}_{i}} \leq E^{esd}_{i,t,s} \leq \overline{E^{esd}_{i}} \tag{34}$$

$$E^{esd}_{i,t_{ini},s} = E^{esd}_{i,t_{end},s} \mid \ t_{ini} = 0 \ \& \ t_{end} = 23 \tag{35}$$

$$\sum_{t\in\Omega_T}(e^{esd^{dch}}_{i,t,s} + e^{esd^{ch}}_{i,t,s}) \leq \Delta^{esd}_{i} \tag{36}$$

$$e^{esd^{dch}}_{i,t,s} - e^{esd^{ch}}_{i,t,s} = e^{esd}_{i,t,s} - e^{esd}_{i,t-1,s} \tag{37}$$

$$0 \leq e^{esd^{dch}}_{i,t,s} \leq 1 \tag{38}$$

$$0 \leq e^{esd^{ch}}_{i,t,s} \leq 1 \tag{39}$$

$$e^{esd}_{i,t,s} \in \{0,1\}$$

$$\forall\, i \in \Omega_{esd}, \forall\, t \in \Omega_t, \forall\, s \in \Omega_s$$

Constraints (31) and (32) define the charge and discharge operation modes of the ESD connected at node i, respectively. The binary variable $e^{esd}_{i,t,s}$ avoids the simultaneous charge/discharge process. The level of stored energy is calculated by (33) and depends on the stored energy level at $t-1$, the charge/discharge efficiencies and the self-discharge rate. The charge level must be within storage capacity limits as shown in (34). In (35) is determined that the charge levels must be equal for the first and the last period. Constraints (36)-(39) limit the operation changes along the 24 hours to preserve the useful life of the ESD.

4.8. Time-of-use Demand Response Program

The TOU demand response program (TOU-DRP) alleviates the pattern consumption of loads at heavy load periods. These modifications decrease overall power losses and improve the quality and reliability of systems [9]. The idea is to change from a heavy load period to a light one, an allowed percentage of demand of customers with whom there is a pre-established agreement. In this way, the overall energy provided to the loads is the same but at more convenient hours. The mathematical model of TOU – DRP is represented by (40)-(44).

$$P^{d/dr}_{i,t,s} = P^{d}_{i}\,\mathfrak{f}_{t,s} + P^{tou^{+}}_{i,t,s} - P^{tou^{-}}_{i,t,s} - P^{ens}_{i,t,s} \tag{40}$$

$$Q^{d/dr}_{i,t,s} = Q^{d}_{i}\,\mathfrak{f}_{t,s} + \tan\theta^{pf}_{i}\,(P^{tou^{+}}_{i,t,s} - P^{tou^{-}}_{i,t,s} - P^{ens}_{i,t,s}) \tag{41}$$

$$0 \leq P^{tou^{+}}_{i,t,s} \leq \mathfrak{Z}^{tou}\cdot P^{d}_{i}\,\mathfrak{f}_{t,s}\cdot \varsigma^{tou}_{i,t,s} \tag{42}$$

$$0 \leq P_{i,t,s}^{tou^-} \leq \mathfrak{Z}^{tou} \cdot P_i^d \, \mathfrak{f}_{t,s} \cdot (1 - \varsigma_{i,t,s}^{tou}) \tag{43}$$

$$\sum_{t \in \Omega_t} P_{i,t,s}^{tou^+} = \sum_{t \in \Omega_t} P_{i,t,s}^{tou^-} \tag{44}$$

$$\varsigma_{i,t,s}^{tou} \in \{0,1\}$$

$$\forall\, i \in \Omega_n, \forall\, t \in \Omega_t, \forall\, s \in \Omega_s$$

The TOU-DRP is applied to modify the load at node i using the positive variables $P_{i,t,s}^{tou^+}$ and $P_{i,t,s}^{tou^-}$, as presented in (40). Besides, it is considered the energy not supplied term ($P_{i,t,s}^{ens}$) that indicates that the real demand at each period can be modified by applying TOU-DRP and the disconnection of a part of the load. In (41) is established that any increase/decrease in the active power demand also affects reactive power demand in the same way, maintaining the power factor of the load. Constraints (42) and (43) limit the increases/decreases of demand at node i to a maximum percentage of the total load given by $\mathfrak{Z}^{tou}$. Notice that the presence of binary variable $\varsigma_{i,t,s}^{tou}$, avoids the simultaneously increase/decrease. Finally, constraint (44) establish that any decrease on load, will be compensated entirely along other day periods.

5. Proposed Neighborhood-based Matheuristic Algorithm

The proposed MISOCP model (1)-(44) is based on a convex formulation with a finite solution that can be solved directly using commercial optimization solvers. However, it is highly complex, impacting the computational time required to find an integer solution. In this sense, alternative solution techniques such as heuristic, metaheuristic, and matheuristic algorithms, for example, are required to solve the problem in large stances.

Matheuristics algorithms are efficient tools that use heuristic strategies and mathematical optimization to decompose and solve highly complex problems [40]. In this paper, we propose a tabu search-based matheuristic approach to solve the MISOCP model (1)-(44). To explore the search space effectively, candidate solutions that move forward in the optimization process need to be generated. These solutions are obtained by making slight modifications to the initial/current solution and are referred to as neighbor solutions. The strategy involves fixing some variables by assigning them a predetermined value or keeping them as variables to be determined by a commercial solver. By doing so, the number of variables in the problem can be reduced, allowing for the solution of sub-models derived from (1)-(44) to obtain neighboring solutions. Since binary and integer variables add complexity to the problem, they are handled using the following neighborhood structures.

5.1. Neighborhood structures

5.1.1. Neighborhood structure for reconfiguration ($\boldsymbol{NB_1}$)

The DNR problem can be handled by generating a set of neighbor radial topologies. In this context, a neighborhood can be obtained through the branch-exchange technique, which has been broadly applied to DNR [41], [42]. The algorithm closes a tie switch forming a closed-loop in the network, and then a sectionalizing switch is opened to recover the radiality of the network.

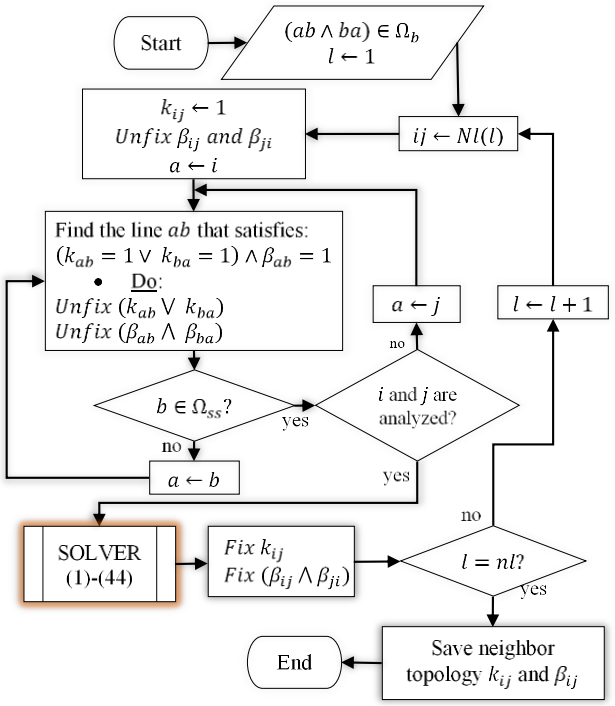

Fig. 2. Neighborhood structure for reconfiguration algorithm (NB_1)

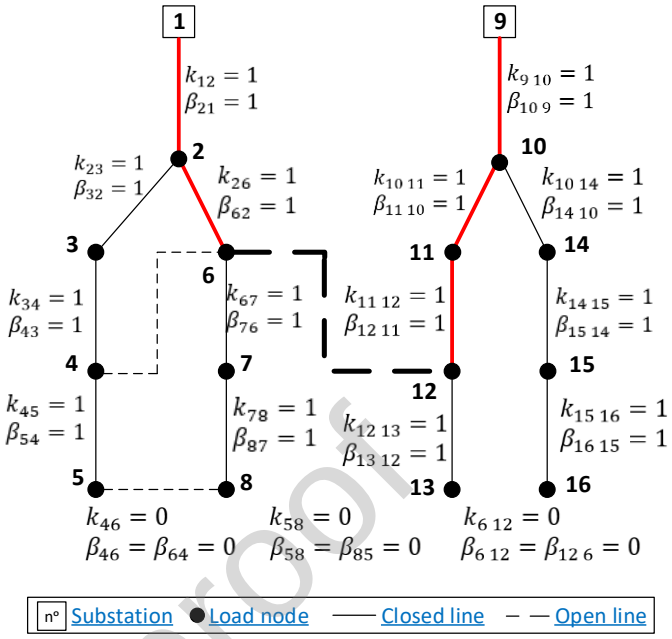

Fig. 3. Closed-loop recognition through k_{ij} and β_{ij} variables.

The proposed branch-exchange algorithm creates radial neighbor topologies by solving reduced submodels of (1)-(44). It removes integer variables of the complete model by the use of k_{ij} and β_{ij}. When an open line ij is closed, i.e., fixing $k_{ij} = 1$, the model is solved just for k_{ij} and β_{ij} of lines that belong to the formed loop. Conversely, the rest of k_{ij} and β_{ij} variables are fixed at their current values. To do that, the algorithm recognizes a formed loop and selects the best line to be opened, as explained in the flowchart of Fig. 2 and the example of Fig. 3.

Fig. 3 shows a didactical system with two substations, three tie switches, and the state of integer variables related to lines. If 6-12 is closed (line in bold), $k_{6\,12}$ is set as 1 and a loop is formed. According to Fig. 2, node i is 6 and the node j is 12, so temporal variable a takes the value 6 and the algorithm finds the line $ab \rightarrow 6b$ or $ba \rightarrow b6$ that is active ($k_{6b\ or\ b6} = 1$) and has the node b as a parent, i.e., $\beta_{6b} = 1$. Among all the variables, just the line 2-6 satisfies the condition since $k_{26} = 1$ and $\beta_{62} = 1$, indicating that 2 is the parent node of 6 and consequently, 2-6 belongs to the closed loop. Since node 2 is not a substation, variable $a = 2$. Now, the algorithm repeats the process to find $2b$ or $b2$ that is active and is a descendant of b. Lines 1-2 and 2-3 are active, however, the parent node of 2 is 1 ($\beta_{21} = 1$), while 3 is a descendant ($\beta_{32} = 1$). At this point, the algorithm recognizes node 1 as a substation, therefore, it is necessary to identify the right side of the loop starting from node j that was assigned as 12. In the same manner, the algorithm identifies the lines that connect node 12 to the substation.

The lines belonging to the closed loop are candidates to be opened and are identified in red. In conclusion, only variables k_{12}, k_{26}, k_{910}, k_{1011}, k_{1112}, β_{12}, β_{21}, β_{26}, β_{62}, β_{910}, β_{109}, β_{1011}, β_{1110}, β_{1112}, and β_{1211} are optimized by solving the MISOCP model (1)-(44) while the rest of the variables k_{ij} and β_{ij} hold fixed on their current values.

It is important to mention that this algorithm is extensible to close several lines at the same time, as indicated in Fig. 2, by the introduction of the vector $Nl_{nl\times 1}$ of dimension $nl \times 1$ where nl indicates the number of lines to be closed to get a neighbor solution.

5.1.2. Neighborhood structure of SCBs ($\boldsymbol{NB_2}$)

The search space of the problem is reduced by fixing the integer variables k_{ij}, β_{ij}, and $e_{i,t,s}^{esd}$ in their current values and including constraints (45) and (46) in the MISOCP model (1)-(44).

$$\hat{n}_{i,t-1,s}^{scb} - \eta \leq n_{i,t,s}^{scb} \leq \hat{n}_{i,t-1,s}^{scb} + \eta \tag{45}$$

$$\sum_{i\in\Omega_{scb}} \hat{n}_{i,t-1,s}^{scb} - \overline{\eta}^{scb} \leq \sum_{i\in\Omega_{scb}} n_{i,t,s}^{scb} \leq \sum_{i\in\Omega_{scb}} \hat{n}_{i,t-1,s}^{scb} + \overline{\eta}^{scb} \tag{46}$$

$$i \in \Omega_{scb,}\ \forall\, t \in \Omega_t, \forall\, s \in \Omega_s$$

Considering the current solution of the NMA for the SCBs operation ($\hat{n}_{i,t,s}^{scb}$), constraint (45) controls the connection or disconnection up to η modules between consecutive scenarios. Similarly, constraint (46) is used to control the number of modules that can be operating in the system, with a bound of $\overline{\eta}^{scb}$ units.

5.1.3. Neighborhood structure of ESDs ($\boldsymbol{NB_3}$)

The operational behavior of the ESDs is represented by the binary variable $e_{i,t,s}^{esd}$ that assumes the values of 1 and 0 for the discharge and charge process, respectively. So the neighborhood structure NB3 is obtained by fixing the integer variables k_{ij}, β_{ij}, and $n_{i,t,s}^{scb}$ in their current values and including constraint (47) in the MISOCP model (1)-(44).

$$\sum_{i\in\Omega_{esd}} e_{i,t-1,s}^{esd} - \overline{\eta}^{esd} \leq \sum_{i\in\Omega_{esd}} e_{i,t,s}^{esd} \leq \sum_{i\in\Omega_{esd}} e_{i,t-1,s}^{esd} + \overline{\eta}^{esd} \tag{47}$$

$$\forall\, t \in \Omega_t, \forall\, s \in \Omega_s$$

Constraint (47) controls the total changes between two consecutive periods. From one period to the next, the maximum changes of operation over all the ESDs, are $\overline{\eta}^{esd}$.

5.2. Matheuristic algorithm

In this section, we delve into the matheuristic approach employed to address the OODSs problem. Firstly, it is important to define the neighbor concept, since it refers to reaching a local optimum state of the network by applying the neighborhood reduction strategies (NB_1, NB_2, NB_3) as in Fig. 4. This process allows the optimization solver to manage the problem within reduced searching spaces easily. NB_1 is first applied due to its greater impact on the solution. Afterward, NB_2 and NB_3 are applied because of their smaller impact. Notice that each neighborhood structure is applied just for its respective kind of variable. Once the topology is defined ($x_k \equiv k_{ij} \cup \beta_{ij} \cup \beta_{ji}$), these variables are fixed, and then SCBs integer variables ($x_{scb} \equiv n_{i,t,s}^{scb}$) are defined. Finally, x_{scb} are fixed to determine ESDs variables ($x_{esd} \equiv e_{i,t,s}^{esd}$).

Simultaneously, a tabu list (TL) for the visited topologies was used in order to implement the concept of memory like on the Tabu Search algorithm. In this regard, each visited topology has an "ol" vector that contains its open switches. The "ol" vector is saved in the "TL" during several iterations defined by the tabu period (TP) parameter, thus avoiding a return to this topology for "TP" iterations.

The search process starts by setting a set of variables to initial values as follows:

- Fix k_{ij} keeping the original topology $\forall ij \in \Omega_b$;
- Relax integrality of taps in SCBs: $n_{i,t,s}^{scb}\ \ \forall i \in \Omega_{scb}$;
- Relax integrality of charge/discharge mode of ESDs: $e_{i,t,s}^{esd}\ \ \forall i \in \Omega_{esd}$;

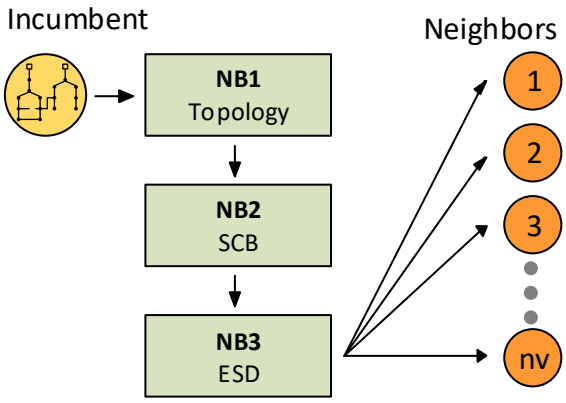

Fig. 4 Algorithm for the creation of neighbor solutions.

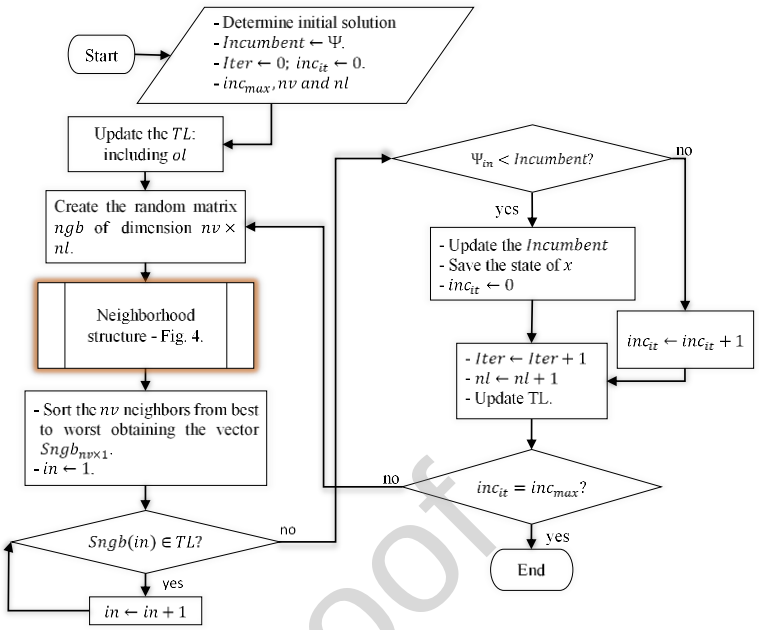

Fig. 5 Proposed Matheuristic algorithm.

- Disable the DRP and the disconnection of load mode: $P_{i,t,s}^{tou+} = P_{i,t,s}^{tou-} = P_{i,t,s}^{ens} = \varsigma_{i,t,s}^{tou} = 0$;
- Solve (1)-(44) through a solver.
- Fix $n_{i,t,s}^{scb}\ \forall i \in \Omega_{scb}$ and $e_{i,t,s}^{esd}\ \forall i \in \Omega_{esd}$, to their closest integer value.

After obtaining the state of the system and the first objective function, the matheuristic proceeds with the process illustrated in the flowchart of Fig. 5. The "$Incumbent$", is a temporal variable that stores the best-found objective function until the current iteration, initially set as the objective function of the initial system state. The "$Iter$" parameter serves aas a counter of iterations, equivalent to the total created neighborhoods. Then, "inc_{it}" parameter counts consecutive iterations where the incumbent is not improved and is used as a stopping criterion. If an "$Incumbent$" is not improved after inc_{max} iterations, the search concludes. "nv" represent the number of neighbors created at each iteration, and "nl" is the number of lines to be closed to apply NB_1. Notice that the vector "ol" contains the open lines of each visited topology.

The search process involves creating a random matrix "$ngb_{(nv\times nl)}$", where each row contains the "nl" lines to be closed, representing "nv" neighbors. Subsequently, the algorithm forms a neighborhood by iteratively closing different "nl" vectors of switches. After a neighborhood is created, it is sorted to create the objective functions vector "$Sngb$" (dimension $nv \times 1$). The algorithm then selects the topology with the best objective function not belonging to the TL and compared its objective function Ψ with the current "$Incumbent$" solution. If it is superior, the "$Incumbent$" is updated; otherwise, it retains its value, and the counter "inc_{it}" increases. Each time the incumbent is updated, the integer and binary variables ($x \equiv x_k \cup x_{scb} \cup x_{esd} \equiv k_{ij} \cup \beta_{ij} \cup \beta_{ji} \cup n_{i,t,s}^{scb} \cup e_{i,t,s}^{esd}$), are saved, and the counter "inc_{it}" is reset. The process halts when the objective function does not improve after "inc_{max}" iterations. As shown in Fig. 5, after each "$Incumbent$" comparison, "nl" increases by one unit diversifying the sear process, and it is reset after reaching a predetermined value avoiding compromising CPU time. This comprehensive process ensures effective exploration of the solution space, making adjustments based on the performance of neighboring solutions while considering the memory-like mechanism of the Tabu List.

As a summarized way, the main elements of the matheuristic proposal presented in Fig. 5 are:

- **Initialization:** The process initiates by setting essential variables and parameters, including the initial topology of the distribution system. The algorithm then proceeds to solve the optimization problem using these initial conditions.
- **Neighborhood Creation:** The algorithm creates a set of neighbors by iteratively closing different sets of lines defined by the "nv" vectors. This represents different potential configurations of the distribution system, considering the state variables such as switch positions and line statuses.
- **Objective Function Evaluation:** For each generated neighborhood, the algorithm evaluates the corresponding objective function. This function encapsulates the key performance metrics relevant to the research question, such as minimizing energy costs, power losses, and ensuring voltage stability.
- **Incumbent Update:** The algorithm maintains an "$Incumbent$" variable, storing the best-found objective function value. If a newly evaluated neighborhood yields a superior solution, the Incumbent is updated, signifying progress toward an optimal operational plan.
- **Memory Mechanism:** To enhance exploration, the algorithm employs a Tabu List, preventing repetition of solutions for a defined period. This mechanism aids in avoiding premature convergence and encourages a more thorough exploration of the solution space.
- **Termination Criteria:** The process continues iteratively until a stopping criterion is met. The algorithm monitors if there is a lack of improvement in the objective function value for a specified number of iterations (as indicated by the "inc_{max}" parameter). This ensures a balance between exploration and exploitation, avoiding unnecessary computational burden.

6. NUMERICAL EXPERIMENTS AND RESULTS

The proposed NMA and MISOCP model were programmed in the mathematical programming language AMPL. For comparative purposes, the commercial solvers GUROBI *v. 9.5.1* and CPLEX *v. 20.1.0.0* are used to perform simulations and both were set with an optimality gap of 1% and a solution time limit of 7 days. A computer with Intel(R) Xeon(R) CPU E5-2650 v4 with a 2.20GHz processor and 64 GB of RAM was used.

The stochastic scenarios obtained, exposed in 4.1, are depicted with data on energy cost, demand, and solar radiation, as presented in Fig. 6, [31]. The cost of CO_2 emissions depends on $\pi^{emis} = 10\ \$/ton$ and the emission factors are $e^{ss} = 2.17$ and $e^{dg} = 0.63$, both in $kg \cdot co_2/kwh$ for Ω_{ss} and Ω_{dg} respectively. The user's reimbursement when applying TOU-DRP, is obtained as 15% of the energy cost at the time of supply, so $\pi^{dr} = 0.15$. Finally, the cost of ENS is $\pi^{ens} = 35\ \$/kwh$.

The parameters of operation are the voltage limits $\overline{V} = 1.05\ p.u.$ and $\underline{V} = 0.95\ p.u.$. The set power factors for Ω_{dg} are $\varphi_i^{c/dg} = \varphi_i^{i/dg} = 0.8$, while for Ω_{pv} are $\varphi_i^{c/pv} = \varphi_i^{i/pv} = 0.9$. Regarding PVs' parameters $T_{amb} = 20$ ºC; $NOCT_i = 45$ ºC and $\delta_i = -0.0045$. The SCBs' switching is limited by $\Delta_i^{scb} = 2$; $\eta = 1$ and $\overline{\eta}^{esd} = 2$. For ESDs: $\overline{P_{i,t,s}^{esd\,ch}} = \overline{P_{i,t,s}^{esd\,dch}} = 800kW$; $\underline{P_{i,t,s}^{esd\,ch}} = \underline{P_{i,t,s}^{esd\,dch}} = 0kW$; $\xi_i^{esd\,ch} = \xi_i^{esd\,dch} = 0.95$; $\xi_i^{esd} = 0.01$; $\Delta_i^{esd} = 2$ and $\overline{\eta}^{esd} = 1$.

6.1. Case studies

The following cases are proposed to assess the application of the TOU-DR program along with network reconfiguration:

- ✓ **Case I:** Initial network topology, neither reconfiguration nor DRP are applied, as detailed in 5.2.

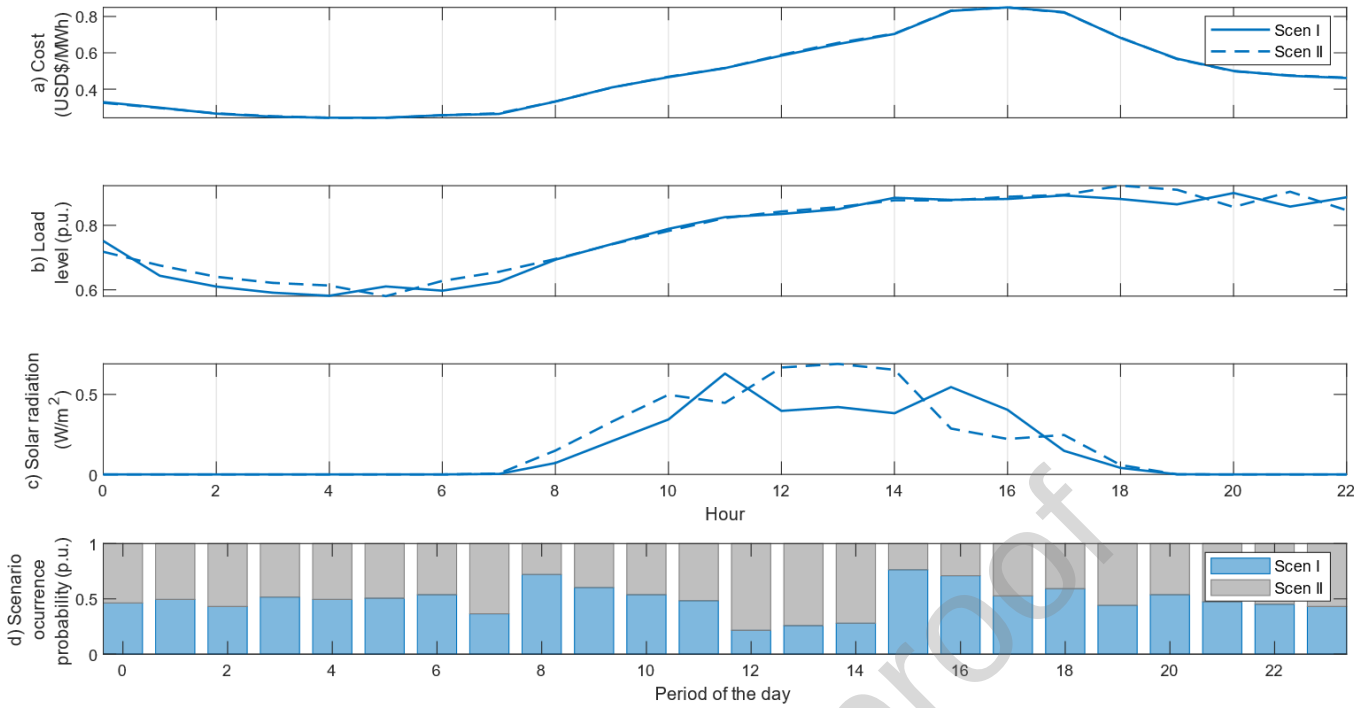

Fig. 6 Stochastic hourly scenarios for parameters: a) Energy costs; b) demand, c) solar irradiation; and d) scenarios occurrence probability.

- ✓ **Case II:** Reconfiguration and DR with $\mathfrak{Z}^{tou} = 0\%$.
- ✓ **Case III:** Reconfiguration and DR with $\mathfrak{Z}^{tou} = 15\%$.
- ✓ **Case IV:** Reconfiguration and DR with $\mathfrak{Z}^{tou} = 30\%$.

6.2. The 69-Bus Distribution System

This distribution system is adapted from [43]. It becomes active with the following DERs: Four DG units of 500 kVA installed at nodes 6, 18, 34, and 61. Four PVs of 500 kVA at nodes 24, 28, 50, and 66. Three ESDs of 1 MVA at nodes 11, 32, and 58. One FCB of 100 kVAr at node 17 and two FCBs of 50 kVAr at nodes 29 and 53, respectively. One SCB with four modeules of 150 kVAr at node 13. The network has five tie switches, and the installed load is $(3{,}802.39 + j\ 2{,}695.60)\ kVA$. The NMA is set with the following values: $nv = 5$, $1 \leq nl \leq 3$, $TL = 5$ and $inc_{max} = 3$.

6.3. The 118-Bus Distribution System

This distribution system is adapted from [44]. It becomes active with the following DERs: Five DG units of 500 kVA at nodes 11, 25, 35, 77, and 104. Four PVs of 1000 kVA at nodes 28, 61, 107, and 111. Three ESDs of 1 MVA at nodes 12, 30, and 87. The set of nodes 9, 30, 48, 57, 58, 59, 73, and 88 are selected to install FCBs of 120 kVAr, two SCBs with four modules of 150 kVAr each at nodes 7 and 73. The network has 14 tie switches, and the installed load is $(22{,}709.72 + j\ 17{,}041.07)\ kVA$. The NMA is set with the values: $nv = 14$, $1 \leq nl \leq 3$, $TL = 10$ and $inc_{max} = 5$.

The number of operation scenarios in the 118-bus system tests has been reduced from 24 to 12. This reduction was necessary as the solver did not provide feasible solutions for the larger scenario set within a reasonable time frame. The scenarios were obtained using the same method described in 4.1. However, to accommodate the reduced number of scenarios, the periods of the day were shortened to twelve intervals.

6.4. Simulations and solutions for the 69-Bus system

For case studies I, II, III, and IV, results are summarized in TABLE 2. Notice the reduction of daily operational costs according to the increase of 3^{tou}. The maximum reduction is achieved in case IV since the objective function is US$ 315.79 cheaper than the network's initial state. On the other hand, variations in the DRP parameter affect the reconfiguration problem since different topologies are determined in each case study. Finally, it should be noted that energy disconnection is only necessary for case IV, which represents the lowest portion of the total cost in the objective function, US$ 5.87. The NMA required a minimum of 15 iterations to solve a case, with a total duration of 43 minutes. Case III represented the longest duration simulation for the NMA, requiring 22 iterations and taking approximately 2.10 hours to solve. Finally, the lowest CPU time is 38.9 minutes for case IV.

The NMA's efficacy is gauged through a comparison with commercial solvers, Gurobi and Cplex. TABLE presents the outcomes of Gurobi and Cplex for cases II, III, and IV. Notably, the NMA consistently outperforms the Gurobi solver in providing superior solutions. However, it is crucial to acknowledge that Cplex achieves more favorable objective functions than the NMA, with objective functions that are 1.83%, 3.5%, and 0.67% smaller respectively. Despite these percentage differences being relatively small, they are noteworthy. In terms of computational efficiency, the NMA emerges as the best. For cases II and III, where solvers operated under a 3-hour time limit, the NMA accomplished the optimization within 2 hours at the worst whilst the most efficient run taking a mere 38 minutes. Conversely, in the case IV, solvers necessitated an extended time limit up to 7 days due to convergence

TABLE 2. RESULTS FOR THE 69 BUS SYSTEM.

	OF ($)	Loss ($)	Emis ($)	DR ($)	ENS ($)	Iter (#)	Time (s)	Open Lines
Case I:	907.08	135.74	771.35	0.00	0.00	--	--	(11,66) (13,21) (15,69) (39,48) (27,54)
Case II:	651.03	64.27	586.75	0.00	0.00	15	2,582.04	(10,11) (12,13) (13,14) (17,18) (47,48)
Case III:	637.00	62.63	559.22	15.15	0.00	22	7,548.17	(10,11) (12,13) (14,15) (17,18) (44,45)
Case IV:	591.29	69.04	490.64	25.74	5.87	20	2,318.97	(5,6) (9,10) (12,13) (13,14) (17,18)

TABLE 3. RESULTS OF SOLVERS FOR THE 69 BUS SYSTEM.

	OF. ($)	Loss ($)	CO2 ($)	DRP ($)	ENS ($)	Time (s)	Open Lines
Case II							
Gurobi	1,648.09	56.79	571.42	0.00	1,019.88	10,800.69	(1,2) (15,16) (47,48) (3,59) (66,67)
Cplex	639.12	70.80	561.85	0.00	6.47	10,895.20	(5,6) (10,11) (14,15) (3,59) (66,67)
Case III							
Gurobi	1,580.46	66.90	572.33	31.51	909.72	10,800.44	(2,3) (4,5) (14,15) (17,18) (59,60)
Cplex	614.73	69.37	530.71	14.36	0.29	10890.33	(4,5) (10,11) (14,15) (51,52) (66,67)
Case IV							
Gurobi	622.21	58.55	535.40	28.27	0	604,802.11	(5,6) (9,10) (12,13) (13,14) (17,18)
Cplex	587.31	61.15	498.84	25.74	1.58	605,053.24	(5,6) (9,10) (12,13) (13,14) (16,17)

challenges. This adjustment was imperative, as the solvers failed to converge within the initial 3-hour limit. Examining the results in Table II and Table III, it is observed that, in case IV, both the NMA and Cplex solvers converged to the same network topology. However, a notable disparity in objective functions was evident. This difference can be ascribed to the superior handling of the TOU-DRP, SCBs, and ESDs scheduling by the Cplex solver.

6.5. Simulations and solutions for the 118-Bus system

Tests and results of the 118-bus system are summarized in TABLE 4. The most significant reduction in daily operational cost, while maintaining the voltage limits $\pm 5\%$, occurs in Case IV, which is at least US$ 272.59 cheaper than the solutions obtained in other cases. Related to the computational performance, the proposed NMA requires 3.04 hours to solve Case III. Notice that number of iterations and the computational time are not related since Case IV employs 22 iterations to converge, although its solution time is lesser than Case III, which converges in 16 iterations. Finally, TABLE 5 shows results obtained by Gurobi and Cplex for Case IV. The proposed NMA is better than the solvers since the objective function and the CPU time to solve this test system are superior. Gurobi requires about 1.24 days to provide a solution, while Cplex takes about seven days (time limit).

Regarding the system performance, Fig. 7 presents the objective function's components for cases II, III, and IV. Notice that the left axis (bars in blue) corresponds to OF and CO_2 emissions, while the right axis (bar in red) corresponds to values of losses, TOU-DRP, and ENS. The decrease in the objective function, CO2 emissions, and losses are minimal among the three cases. This indicates that the reconfiguration process significantly impacts the overall objective function, while the demand response program (DRP) has a minor influence on the daily operation. TOU-DRP's cost is the smaller part of objective function, although their impact on peak load relaxation is relevant. On the other hand, ENS cost is reduced to US$ 178.62 in Case IV. It is important to mention that the portion of demand not supplied is an emergency option in case of voltage instability and overload. At the bottom of Fig. 7, the minimum

TABLE 4. RESULTS FOR THE 118 BUS SYSTEM.

	OF ($)	Loss ($)	Emis ($)	DR ($)	ENS ($)	Iter (#)	Time (s)	Open Lines
Case I:	8,740.94	737.55	8,003.39	0.00	0.00	--	--	(46,27) (17,27) (8,24) (54,43) (62,49) (37,62) (9,40) (58,96) (73,91) (88,75) (99,77) (108,83) (105,86) (110,118)
Case II:	9,091.29	484.59	7,958.90	0.00	647.80	10	2,523.04	(22,23) (34,35) (39,40) (42,43) (53,54) (57,58) (70,71) (97,98) (117,118) (17,27) (58,96) (73,91) (108,83) (105,86)
Case III:	9,053.58	469.57	7,783.08	59.06	741.86	13	5,548.17	(16,17) (22,23) (34,35) (39,40) (42,43) (52,53) (57,58) (70,71) (58,96) (88,75) (99,77) (108,83) (105,86) (110,118)
Case IV:	8,780.99	465.25	8,025.03	112.09	178.62	10	1,518.97	(16,17) (21,22) (34,35) (39,40) (42,43) (53,54) (61,62) (71,72) (87,88) (91,96) (97,98) (109,110) (108,83) (105,86)

TABLE 5. RESULTS OF SOLVERS FOR CASE IV - 118 BUS SYSTEM.

	OF. ($)	Loss ($)	CO2 ($)	DRP ($)	ENS ($)	Time (*s*)	Open Lines
Gurobi	8,805.43	466.98	8033.70	112.39	192.35	123,058.21	(21,22) (24,25) (34,35) (39,40) (42,43) (51,52) (61,62) (70,71) (82,83) (86,87) (91,96) (97,98) (109,110) (105,86)
Cplex	8,798.44	473.00	8058.76	113.16	153.53	604,803.33	(23,24) (24,25) (34,35) (39,40) (42,43) (51,52) (61,62) (71,72) (74,75) (75,76) (79,86) (91,96) (109,110) (108,83)

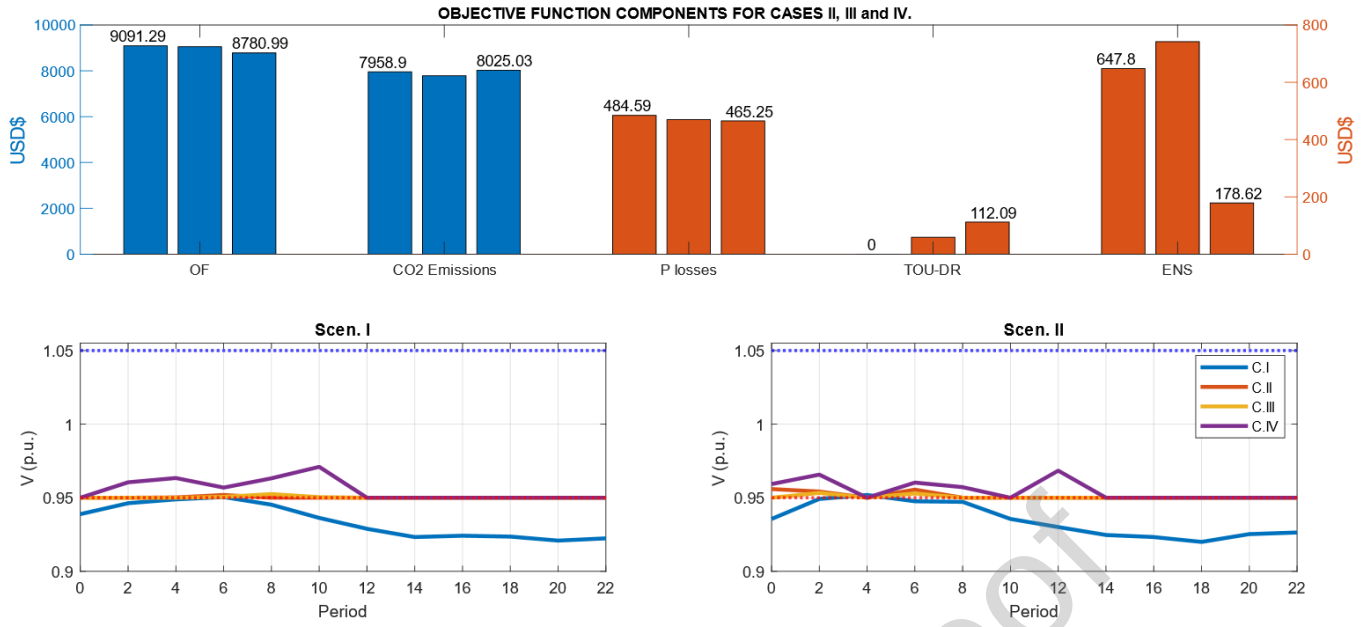

Fig. 7. Objective function values at cases II, III and IV respectively. Below, minimum voltages profile of each case of study.

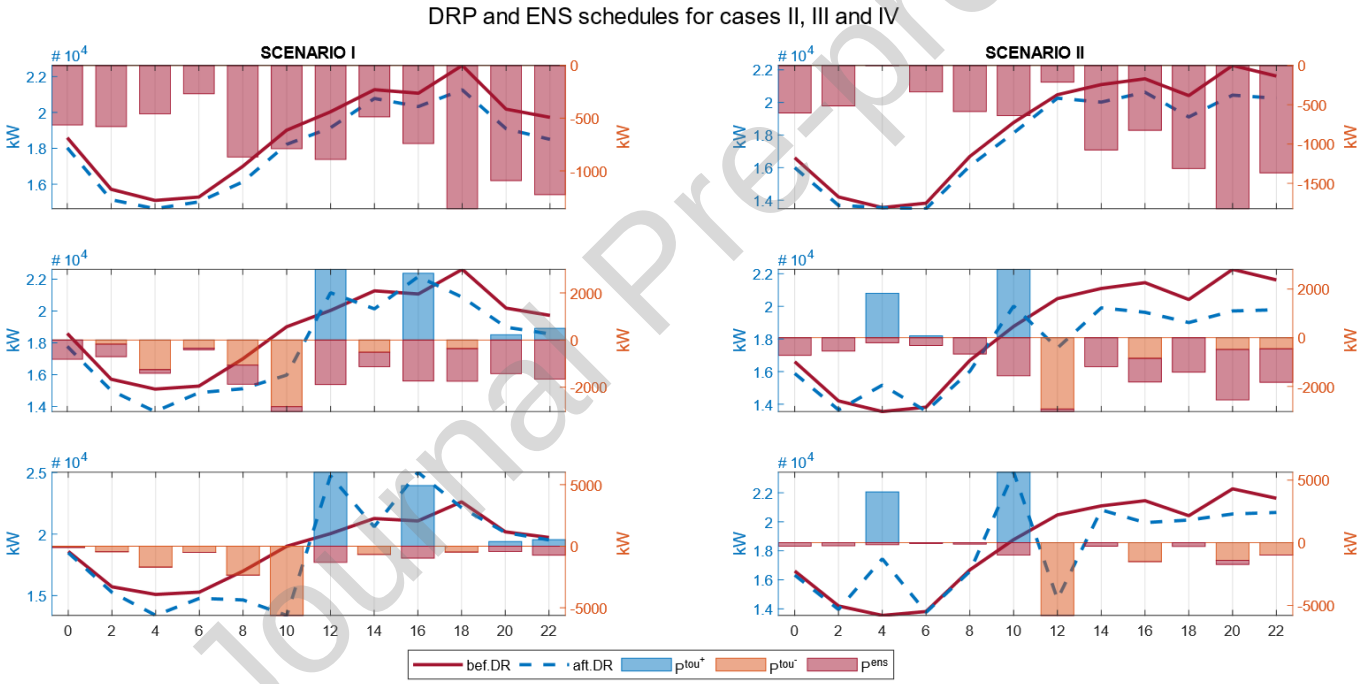

Fig. 8. Active power schedule of TOU-DRP and ENS for cases II, III and IV.

voltage profiles are presented. Significant improvements can be observed in the minimum voltage profile compared to Case I, particularly in Case IV, where the voltage values are notably better.

Fig. 9 shows, in each row, the TOU-DRP and ENS applications for cases II, III, and IV, respectively. The profiles of not supplied power and power increases/decreases of the DRP are plotted in bars, and line plots represent the demand before and after the TOU-DRP application. There is a significant reduction of demand in cases III and IV for scenario II, which occurs in peak hours (from 12h). Considering the scenario I and cases III and IV, the demand profile is slighter, and the reduction occurs between 0h and 10h. Notice the relevant substitution of ENS with TOU-DRP between cases III and IV. Finally, Fig. 9 depicts the active power injections of DGs, PVs, and ESDs. For all the cases, DGs are working close to their maximum

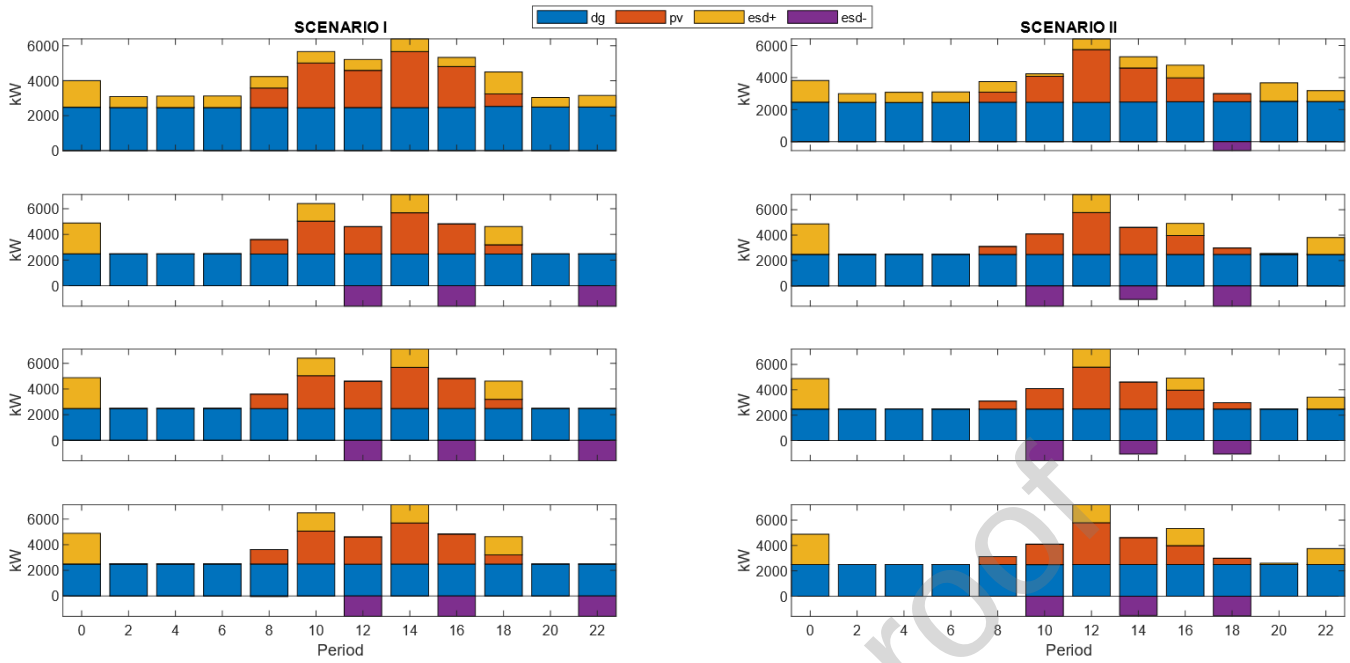

Fig. 9. Active power schedule of DERs installed at the system, cases I, II, III and IV.

capacity to contribute to the reduction of SE's participation. PV's injection is significant, especially at 12h and 14h, and during the PVs' injection periods, it is produced the ESDs charge.

7. CONCLUSIONS

This work presents a mixed-integer second-order cone programming model to optimize the daily operational cost of distribution systems through network reconfiguration and the optimal control of distributed energy resources, energy storage, and switchable capacitor banks. A stochastic scenario-based approach represents a typical day of a year's season. Besides, the proposed model includes a time-of-use demand response program (TOU-DRP). On the other hand, due to the complexity of the problem, a neighborhood-based matheuristic approach (NMA) based on tabu search was designed to solve the problem. This approach enabled the solution of problems of planning the operation of distribution systems currently in operation, considering a large number of integer and discrete variables, with reliable quality in an adequate computational time. This performance is not possible using only classical mathematical optimization or metaheuristics techniques, given their limitations for analyzing the problem solution search space. The NMA was successfully validated by comparing it with two commercial solvers, providing high-quality solutions with less computational effort. Results suggest that using a commercial solver to perform a neighborhood search generates efficient optimization tools.

Results reveal that relaxing the demand profile is convenient to alleviate the system at peak hours and leads to important reductions of the objective function compared with initial states that do not consider a TOU-DRP option. Moreover, results also show that the network topology of the system changes along with the variation of the TUO-DRP.

As future work, analysis can be addressed within a DRP framework, considering constraints of aggregators and type of loads. In the same way, electric vehicles can be added to the analysis to take advantage of energy storage devices.

8. ACKNOWLEDGMENT

This work was supported in part by the Coordination for the Improvement of Higher Education Personnel (CAPES) – Finance Code 001, in part by the Brazilian National Council for Scientific and Technological Development (CNPq), 304726/2020-6, in part by the São Paulo Research Foundation (FAPESP), under grants 2015/21972-6, 2019/01841-5, and 2019/23755-3.

9. REFERENCES

[1] L. Li y S. Yu, «Optimal management of multi-stakeholder distributed energy systems in low-carbon communities considering demand response resources and carbon tax», *Sustainable Cities and Society*, vol. 61, p. 102230, oct. 2020.

[2] J. M. Home-Ortiz, M. Pourakbari-Kasmaei, M. Lehtonen, y J. R. Sanches Mantovani, «Optimal location-allocation of storage devices and renewable-based DG in distribution systems», *Electric Power Systems Research*, vol. 172, pp. 11-21, jul. 2019.

[3] A. J. Chapman y K. Itaoka, «Energy transition to a future low-carbon energy society in Japan's liberalizing electricity market: Precedents, policies and factors of successful transition», *Renewable and Sustainable Energy Reviews*, vol. 81, pp. 2019-2027, ene. 2018.

[4] G. Barone, A. Buonomano, C. Forzano, G. F. Giuzio, y A. Palombo, «Increasing renewable energy penetration and energy independence of island communities: A novel dynamic simulation approach for energy, economic, and environmental analysis, and optimization», *Journal of Cleaner Production*, vol. 311, p. 127558, ago. 2021.

[5] Y. Wang, J. Qiu, Y. Tao, X. Zhang, y G. Wang, «Low-carbon oriented optimal energy dispatch in coupled natural gas and electricity systems», *Applied Energy*, vol. 280, p. 115948, dic. 2020.

[6] S. Zhang, W. Hu, J. Du, C. Bai, W. Liu, y Z. Chen, «Low-carbon optimal operation of distributed energy systems in the context of electricity supply restriction and carbon tax policy: A fully decentralized energy dispatch strategy», *Journal of Cleaner Production*, vol. 396, p. 136511, abr. 2023.

[7] M. J. Ghadi, S. Ghavidel, A. Rajabi, A. Azizivahed, L. Li, y J. Zhang, «A review on economic and technical operation of active distribution systems», *Renewable and Sustainable Energy Reviews*, vol. 104, pp. 38-53, abr. 2019.

[8] T. S. Vitor y J. C. M. Vieira, «Operation planning and decision-making approaches for Volt/Var multi-objective optimization in power distribution systems», *Electric Power Systems Research*, vol. 191, p. 106874, feb. 2021.

[9] M. A. Tavakoli Ghazi Jahani, P. Nazarian, A. Safari, y M. R. Haghifam, «Multi-objective optimization model for optimal reconfiguration of distribution networks with demand response services», *Sustainable Cities and Society*, vol. 47, p. 101514, may 2019.

[10] L. H. Macedo, J. F. Franco, M. J. Rider, y R. Romero, «Optimal Operation of Distribution Networks Considering Energy Storage Devices», *IEEE Trans. Smart Grid*, vol. 6, n.º 6, pp. 2825-2836, nov. 2015.

[11] P. P. Vergara, J. C. López, M. J. Rider, H. R. Shaker, L. C. P. da Silva, y B. N. Jørgensen, «A stochastic programming model for the optimal operation of unbalanced three-phase islanded microgrids», *International Journal of Electrical Power & Energy Systems*, vol. 115, p. 105446, feb. 2020.

[12] S. A. Mansouri *et al.*, «A multi-stage joint planning and operation model for energy hubs considering integrated demand response programs», *International Journal of Electrical Power & Energy Systems*, vol. 140, p. 108103, sep. 2022.

[13] V. Maniezzo, M. A. Boschetti, y T. Stützle, *Matheuristics: Algorithms and Implementations*. en EURO Advanced Tutorials on Operational Research. Cham: Springer International Publishing, 2021.

[14] D. Schermer, M. Moeini, y O. Wendt, «A matheuristic for the vehicle routing problem with drones and its variants», *Transportation Research Part C: Emerging Technologies*, vol. 106, pp. 166-204, sep. 2019.

[15] R. Turkeš, K. Sörensen, y D. P. Cuervo, «A matheuristic for the stochastic facility location problem», *J Heuristics*, vol. 27, n.º 4, pp. 649-694, ago. 2021.

[16] S. H. Alemohammad, E. Mashhour, y M. Saniei, «A market-based method for reconfiguration of distribution network», *Electric Power Systems Research*, vol. 125, pp. 15-22, ago. 2015.

[17] C. L. B. Silveira, A. Tabares, L. T. Faria, y J. F. Franco, «Mathematical optimization versus Metaheuristic techniques: A performance comparison for reconfiguration of distribution systems», *Electric Power Systems Research*, vol. 196, p. 107272, jul. 2021.

[18] O. Badran, S. Mekhilef, H. Mokhlis, y W. Dahalan, «Optimal reconfiguration of distribution system connected with distributed generations: A review of different methodologies», *Renewable and Sustainable Energy Reviews*, vol. 73, pp. 854-867, jun. 2017.

[19] R. A. Jabr, R. Singh, y B. C. Pal, «Minimum Loss Network Reconfiguration Using Mixed-Integer Convex Programming», *IEEE Trans. Power Syst.*, vol. 27, n.º 2, pp. 1106-1115, may 2012.

[20] Z. Tian, W. Wu, B. Zhang, y A. Bose, «Mixed-integer second-order cone programing model for VAR optimisation and network reconfiguration in active distribution networks», *IET Generation, Transmission & Distribution*, vol. 10, n.º 8, pp. 1938-1946, may 2016.

[21] J. M. Home-Ortiz, R. Vargas, L. H. Macedo, y R. Romero, «Joint reconfiguration of feeders and allocation of capacitor banks in radial distribution systems considering voltage-dependent models», *International Journal of Electrical Power & Energy Systems*, vol. 107, pp. 298-310, may 2019.

[22] J. F. Franco, M. J. Rider, M. Lavorato, y R. Romero, «A mixed-integer LP model for the reconfiguration of radial electric distribution systems considering distributed generation», *Electric Power Systems Research*, vol. 97, pp. 51-60, abr. 2013.

[23] O. Benmiloud, B. E. Daoudi, y S. Arif, «Reconfiguration of Distribution Power Systems for Optimal Operation», *Signal Processing*, p. 6, 2017.

[24] A. Zare Ghaleh Seyyedi, E. Akbari, M. H. Atazadegan, S. Mahmoudi Rashid, A. Niazazari, y S. Shahmoradi, «A stochastic tri-layer optimization framework for day-ahead scheduling of microgrids using cooperative game theory approach in the presence of electric vehicles», *Journal of Energy Storage*, vol. 52, p. 104719, ago. 2022.

[25] S. F. Santos, D. Z. Fitiwi, M. R. M. Cruz, C. M. P. Cabrita, y J. P. S. Catalão, «Impacts of optimal energy storage deployment and network reconfiguration on renewable integration level in distribution systems», *Applied Energy*, p. 12, 2017.

[26] F. Sheidaei, A. Ahmarinejad, M. Tabrizian, y M. Babaei, «A stochastic multi-objective optimization framework for distribution feeder reconfiguration in the presence of renewable energy sources and energy storages», *Journal of Energy Storage*, vol. 40, p. 102775, ago. 2021.

[27] M. Sedighizadeh, G. Shaghaghi-shahr, M. Esmaili, y M. R. Aghamohammadi, «Optimal distribution feeder reconfiguration and generation scheduling for microgrid day-ahead operation in the presence of electric vehicles considering uncertainties», *Journal of Energy Storage*, vol. 21, pp. 58-71, feb. 2019.

[28] Q. Chen, W. Wang, H. Wang, J. Wu, y J. Wang, «An Improved Beetle Swarm Algorithm Based on Social Learning for a Game Model of Multiobjective Distribution Network Reconfiguration», *IEEE Access*, vol. 8, pp. 200932-200952, 2020.

[29] J. M. Home-Ortiz, M. Pourakbari Kasmaei, M. Lehtonen, y J. R. Sanches Mantovani, «A Mixed Integer Conic Model for Distribution Expansion Planning», mar. 2020.

[30] J. M. Home-Ortiz, W. C. De Oliveira, y J. R. S. Mantovani, «Optimal Power Flow Problem Solution through a Matheuristic Approach», *IEEE Access*, vol. 9, pp. 84576-84587, 2021.

[31] J. G. Y. Romero, J. M. Home-Ortiz, M. S. Javadi, M. Gough, J. R. S. Mantovani, y J. P. S. Catalão, «Matheuristic Algorithm Based on Neighborhood Structure to Solve the Reconfiguration Problem of Active Distribution Systems», en *2021 IEEE International Conference on Environment and Electrical Engineering and 2021 IEEE Industrial and Commercial Power Systems Europe (EEEIC / I CPS Europe)*, sep. 2021, pp. 1-6.

[32] K. Ullah, G. Hafeez, I. Khan, S. Jan, y N. Javaid, «A multi-objective energy optimization in smart grid with high penetration of renewable energy sources», *Applied Energy*, vol. 299, p. 117104, oct. 2021.

[33] D. Syed *et al.*, «Deep Learning-Based Short-Term Load Forecasting Approach in Smart Grid With Clustering and Consumption Pattern Recognition», *IEEE Access*, vol. 9, pp. 54992-55008, 2021.

[34] G. Grigoraș *et al.*, «Contributions to Power Grid System Analysis Based on Clustering Techniques», *Sensors*, vol. 23, n.º 4, Art. n.º 4, ene. 2023.

[35] C. Si, S. Xu, C. Wan, D. Chen, W. Cui, y J. Zhao, «Electric Load Clustering in Smart Grid: Methodologies, Applications, and Future Trends», *Journal of Modern Power Systems and Clean Energy*, vol. 9, n.º 2, pp. 237-252, mar. 2021.

[36] J. Han, J. Pei, y M. Kamber, *Data Mining: Concepts and Techniques*. Elsevier, 2011.

[37] L. Baringo y A. J. Conejo, «Correlated wind-power production and electric load scenarios for investment decisions», *Applied Energy*, vol. 101, pp. 475-482, ene. 2013.

[38] J. F. Franco, M. J. Rider, y R. Romero, «A mixed-integer quadratically-constrained programming model for the distribution system expansion planning», *International Journal of Electrical Power & Energy Systems*, vol. 62, pp. 265-272, nov. 2014.

[39] S. Montoya-Bueno, J. I. Munoz, y J. Contreras, «A Stochastic Investment Model for Renewable Generation in Distribution Systems», *IEEE Trans. Sustain. Energy*, vol. 6, n.º 4, pp. 1466-1474, oct. 2015.

[40] M. Fischetti y M. Fischetti, «Matheuristics», en *Handbook of Heuristics*, R. Martí, P. M. Pardalos, y M. G. C. Resende, Eds., Cham: Springer International Publishing, 2018, pp. 121-153.

[41] D. W. Ross, M. Carson, y R. Nuytten, «Development of advanced methods for planning electric energy distribution systems. Volume 2. Software documentation. Final report. [SWITCH-1 and DISOPT-1 codes]», Systems Control, Inc., Palo Alto, CA (USA), SCI-5263(Vol.2), dic. 1979.

[42] M. E. Baran y F. F. Wu, «Network reconfiguration in distribution systems for loss reduction and load balancing», *IEEE Trans. Power Delivery*, vol. 4, n.º 2, pp. 1401-1407, abr. 1989.

[43] M. E. Baran y F. F. Wu, «Optimal capacitor placement on radial distribution systems», *IEEE Trans. Power Delivery*, vol. 4, n.º 1, pp. 725-734, ene. 1989.

[44] A. R. Abul'Wafa, «Ant-lion optimizer-based multi-objective optimal simultaneous allocation of distributed generations and synchronous condensers in distribution networks», *International Transactions on Electrical Energy Systems*, vol. 29, n.º 3, p. e2755, 2019.

Credit author statement

Jairo Yumbla: Conceptualization, Methodology, Software, Writing.
Juan M. Home-Ortiz: Conceptualization, Methodology, Software, Writing.
Tiago Pinto: Writing, Supervision, Reviewing.
João P. S. Catalão: Supervision, Reviewing.

José Roberto Sanches Mantovani: Supervision, Reviewing.

Declaration of Competing Interest

☒ The authors declare that they have no known competing financial interests or personal relationships that could have appeared to influence the work reported in this paper.

☐ The authors declare the following financial interests/personal relationships which may be considered as potential competing interests: